Journal of Crystal Growth 347 (2012) 95–98

Contents lists available at SciVerse ScienceDirect

Journal of Crystal Growth

journal homepage: www.elsevier.com/locate/jcrysgro

Degenerated MgZnO films obtained by excessive zinc

J.S. Liu [a,b], C.X. Shan [a,*], S.P. Wang [a], B.H. Li [a], Z.Z Zhang [a], D.Z. Shen [a]

[a] State Key Laboratory of Luminescence and Applications, Changchun Institute of Optics, Fine Mechanics and Physics, Chinese Academy of Sciences, 3888 Dongnanhu Road, Changchun 130033, People's Republic of China

[b] Graduate University of the Chinese Academy of Sciences, Beijing 100049, People's Republic of China

ARTICLE INFO

Article history:
Received 2 January 2012
Received in revised form
26 February 2012
Accepted 13 March 2012
Communicated by D.P. Norton
Available online 20 March 2012

Keywords:
A1. Characterization
A3. Molecular beam epitaxy
B2. Semiconducting II–VI materials

ABSTRACT

By introducing excessive zinc during the growth process, degenerated $Mg_{0.46}Zn_{0.54}O$ films have been prepared. The resistivity of the $Mg_{0.46}Zn_{0.54}O$ films is only 0.053 Ω cm, and the electron concentration is 1.0×10^{19} cm^{-3}, which is well above the Mott concentration of ZnO (2.9×10^{18} cm^{-3}). The origin of such a high electron concentration can be attributed to the excessive zinc in the films. The results reported in this paper provide a route to conductive degenerated MgZnO films, thus may lay a ground for the fabrication of ZnO-based heterostructures or deep ultraviolet optoelectronic devices.

1. Introduction

A degenerated semiconductor is a semiconductor with such a high carrier concentration that the material starts to act more like a metal. Since generated semiconductors are highly conductive, they are necessary in a variety of applications in optoelectronic devices [1]. Ultraviolet semiconductor optoelectronic devices have potential applications in information storage, air and water sterilization, biology and medical therapeutics, etc. [2,3]. Zinc oxide (ZnO) has been a promising candidate for the aforementioned applications for its unique properties such as large bandgap (3.37 eV), large exciton binding energy (60 meV), abundance, and bio-compatibility [4,5]. In many cases, the optoelectronic devices are fabricated from heterostructures by a proper bandgap engineering. For the fabrication of heterostructures, larger bandgap materials acting as a counterpart of ZnO are usually indispensable. MgZnO has been considered as a suitable candidate for such a counterpart for its large bandgap and small lattice-mismatch with ZnO [6]. Also by alloying with MgO, the bandgap of ZnO can be extended to the deep ultraviolet region (with wavelength shorter than 300 nm); thus deep ultraviolet devices may be realized from MgZnO-based semiconductors [7–9]. In order to develop ZnO-based heterostructures and deep ultraviolet devices, one important issue is to fabricate conductive or even degenerated MgZnO films. Nevertheless, with increasing Mg content, the conductivity of MgZnO decreases drastically. Therefore, it is of great importance and significance if highly conductive degenerated MgZnO films can be prepared. To realize conductive ZnO-based materials, group III elements such as Ga and Al have been adopted as donor dopants [10,11]. Although many reports on group III elements doped ZnO films have been prepared, no report on degenerated MgZnO films can be found to date.

In this letter, by introducing excessive zinc during the growth process, degenerated $Mg_{0.46}Zn_{0.54}O$ films have been prepared. The carrier concentration in the films is as high as 1.0×10^{19} cm^{-3}, which is well above the Mott concentration of ZnO (2.9×10^{18} cm^{-3}). Such a high carrier concentration MgZnO films have not been reported before.

2. Experiment

The MgZnO films were grown on *a*-plane sapphire substrates in a plasma-assisted molecular beam epitaxy technique. Elemental zinc (6 N) and magnesium (5 N) contained in Knudsen cells were employed as precursors of the MgZnO films, and atomic oxygen generated from O_2 gas (5 N) via a 13.56 MHz radio frequency plasma cell operated at 300 W was employed as the oxygen source. Before growth, the substrate was treated by oxygen plasma at 600 °C for 10 min to produce an oxygen-terminated surface. During the growth process, the pressure in the growth chamber was fixed at 2×10^{-5} mbar, and the substrate temperature at 600 °C. To obtain excess zinc in MgZnO, the growths were conducted intentionally in a zinc-rich condition. In

* Corresponding author. Tel./fax: +86 43186176298.
E-mail addresses: phycxshan@yahoo.com.cn (C.X. Shan), dzshen824@sohu.com (D.Z. Shen).

0022-0248/$ - see front matter © 2012 Elsevier B.V. All rights reserved.
http://dx.doi.org/10.1016/j.jcrysgro.2012.03.028

this way, MgZnO films with a thickness of 600 nm have been prepared.

The structure characterization of the films was carried out in a Bruker D8 X-ray diffractometer (XRD) with CuKα ($\lambda = 1.54$ Å) as the excitation source. The absorption spectra of the MgZnO films were recorded in a Shimadzu UV-3101PC scanning spectrophotometer. The electrical properties of the films were measured in a Hall measurement system (Lakeshore 7707). Temperature-dependent Hall measurement was conducted over the temperature range from 85 to 400 K using a continuous flow liquid nitrogen cooling system. The composition of the MgZnO films was determined by energy-dispersive X-ray spectroscopy.

3. Results and discussion

The Mg content in the MgZnO films determined by energy-dispersive X-ray spectroscopy is 0.46. The typical XRD patterns of the $Mg_{0.46}Zn_{0.54}O$ films are shown in Fig. 1. Only one strong peak at 34.9° can be observed in the θ–2θ powder diffraction pattern besides the peak from the substrate, which can be indexed to the diffraction from hexagonal MgZnO (0002) facets. The powder diffraction data reveal that the films are crystallized in hexagonal phase with (0002) preferred orientation. The X-ray rocking curve of the films displays a good symmetric Gaussian lineshape, and the full width at half maximum of the curve is 1883 arcsec, as shown in Fig. 1(b). X-ray phi-scan analysis of the films is shown in Fig. 1(c), and six well-defined peaks with 60° interval can be observed in the pattern, which indicates that the films have a six-fold symmetry.

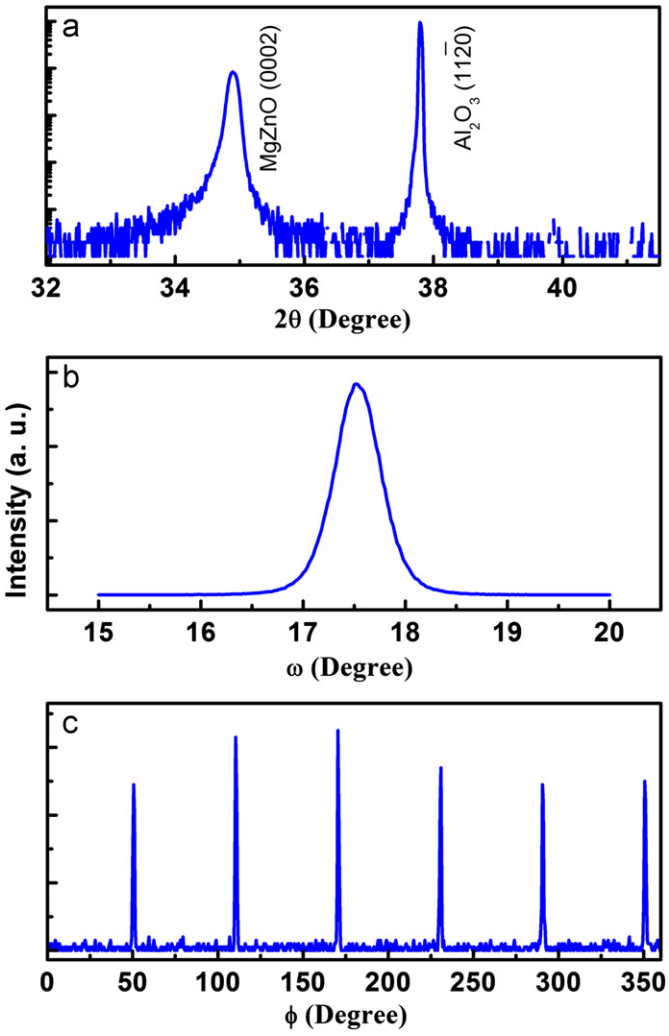

Fig. 1. $\theta-2\theta$ XRD spectrum (a), the (0002) X-ray rocking curve (b) and the phi-scan (102) reflection (c) of the $Mg_{0.46}Zn_{0.54}O$ films.

The Hall measurement shows that the room temperature electron concentration of the $Mg_{0.46}Zn_{0.54}O$ film is 1.0×10^{19} cm^{-3}, the mobility of the film is 10.6 cm^2/V s, and the resistivity of the film is 0.053 Ω cm. In order to confirm the high conductivity of the film, temperature-dependent electrical properties of the $Mg_{0.46}Zn_{0.54}O$ film were studied, as shown in Fig. 2. Interestingly, the electron concentration of the film is almost independent of temperature in the investigated range from 85 to 400 K, as shown in Fig. 2(a). This symbolizes that the $Mg_{0.46}Zn_{0.54}O$ film may be degenerated. To be degenerated, the Mott transition carrier concentration has to be reached. The Mott transition carrier concentration n in a condensed matter can be expressed by the following equation [12]:

$$n \simeq (0.2/a_H)^3 \quad (1)$$

where a_H is the exciton Bohr radius. For ZnO, the exciton Bohr radius is 1.4 nm [13]; then the Mott transition carrier concentration of ZnO obtained from Eq. (1) is about 2.9×10^{18} cm^{-3}. Note that the electron concentration in our MgZnO films (1.0×10^{19} cm^{-3}) is well above the Mott transition electron concentration, the $Mg_{0.46}Zn_{0.54}O$ film is degenerated, and thus the electron concentration in the film is almost independent of temperature.

Temperature-dependent mobility also confirms the degenerate nature of the $Mg_{0.46}Zn_{0.54}O$ films, as shown in Fig. 2(b). Generally, three major types of scattering mechanisms are the limiting factors that determine the mobility of an alloy semiconductor. (I) Impurity scattering, which arises from the scattering caused by the impurities in the material. The ionized impurity scattering of carriers depends on temperature as $\mu_{II} \propto T^{1.5}$.

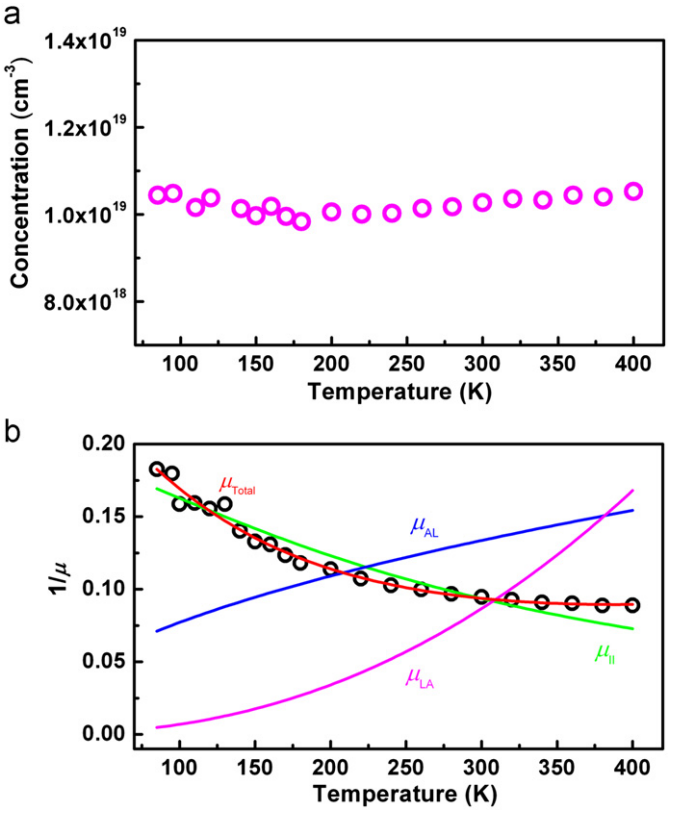

Fig. 2. Temperature-dependence electron concentration (a) and mobility data (b) of the $Mg_{0.46}Zn_{0.54}O$ films obtained by Hall measurement, and the solid lines in (b) are fittings to the scattered experimental data.

However, in the case of degenerate semiconductors, the equation should be modified as $\mu_{II}=C+AT^{1.5}$, where C is the constant mobility that will be approached as the temperature goes to zero, and A is the proportionality factor for the ionized impurity scattering [14]. (II) Lattice scattering, which results from the thermal motion of the lattice atoms at temperature above 0 K; the agitation of the atoms causes variations in the potential resulting in the emission of phonons which transfer energy between the lattice and the free carriers. The mobility due to lattice scattering depends on temperature by the following expression: $\mu_{LA}\propto T^{-1.5}$. (III) Alloy scattering—this type of scattering occurs in alloys. The alloy scattering depends on temperature can be written as $\mu_{AL}\propto T^{-0.5}$ [15]. The total mobility of an alloy material considering the three abovementioned scattering factors can be approximated according to Matthiessen's rule: $\mu_{Total}^{-1}=\mu_{II}^{-1}+\mu_{AL}^{-1}+\mu_{LA}^{-1}$. It is found that the fitting curve agrees fairly well with the factor of ionized impurity scattering μ_{II} in a degenerated semiconductor, as shown in Fig. 2(b). Therefore, the temperature-dependent mobility data further confirm that the films are degenerated. Note that there have been some reports on degenerated ZnO [16–18], but no previous report on degenerated MgZnO can be found. We note that the preparation of the degenerated MgZnO films is not occasional because over three samples have been grown under identical conditions, and similar results have been obtained.

The absorption spectrum of the degenerated $Mg_{0.46}Zn_{0.54}O$ film is shown in Fig. 3. The film shows a sharp absorption edge at around 290 nm. To evaluate the bandgap (E_g) of the films, we employed a $\alpha^2\propto(h\nu-E_g)$ expression to fit the absorption spectrum of the $Mg_{0.46}Zn_{0.54}O$ films [6], where α is the absorption coefficient and $h\nu$ is the photon energy. Hence, the bandgap for the $Mg_{0.46}Zn_{0.54}O$ films deduced from the absorption spectrum is about 4.344 eV. Meanwhile, it has been demonstrated that the dependence of the bandgap of wurtzite structured $Mg_xZn_{1-x}O$ $E_g(Mg_xZn_{1-x}O)$ on its composition can be expressed by the following formula [19]:

$$E_g(Mg_xZn_{1-x}O)=3.384+1.705x \quad (2)$$

where x is the Mg composition in the $Mg_xZn_{1-x}O$ film. By inserting the Mg composition of 0.46 into Eq. (2), a bandgap value of 4.168 eV can be derived. Note that this value is noticeably smaller than the one obtained from the absorption spectrum (4.344 eV). The above phenomenon indicates that some zinc

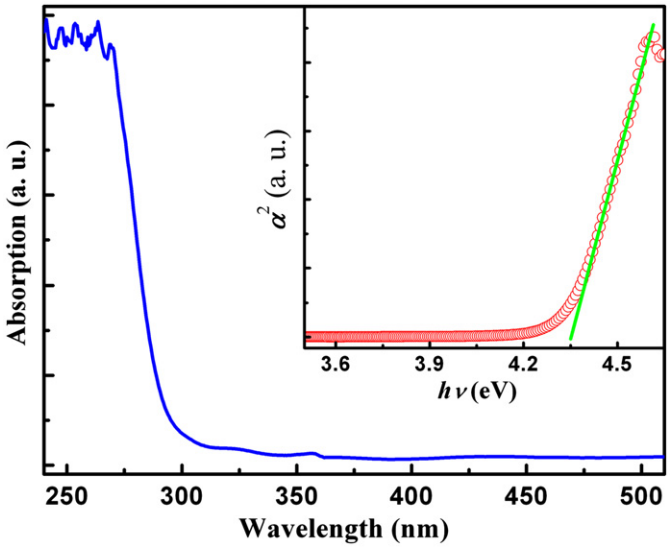

Fig. 3. Absorption spectrum of the $Mg_{0.46}Zn_{0.54}O$ films, and the inset shows the bandgap determined from the absorption spectrum.

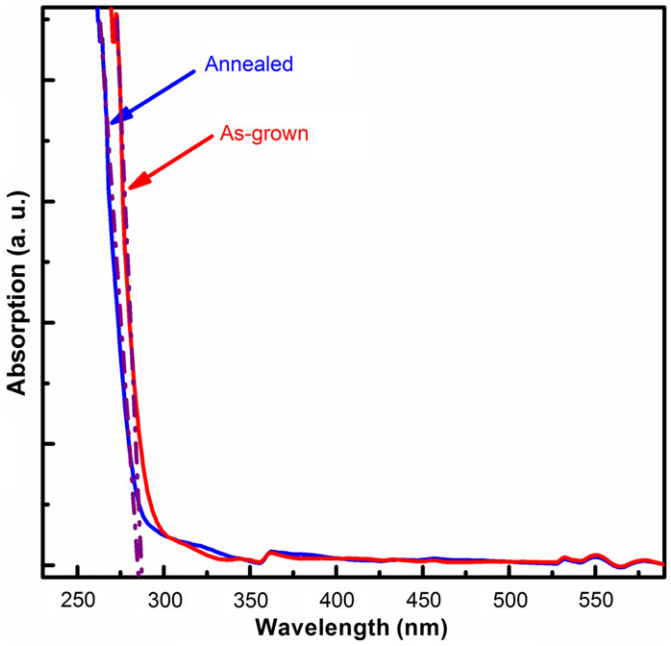

Fig. 4. Absorption spectra of the as-grown and annealed MgZnO films.

contents do not contribute to the bandgap of the $Mg_{0.46}Zn_{0.54}O$ film. It has been demonstrated that the excess zinc might occupy the interstitial sites, and the interstitial zinc may contribute to the conduction of ZnO based films [20]. Therefore, it is presumed that the high electron concentration in the MgZnO films obtained in our experiment may be caused by the excess zinc.

To test the above presumption, the films were annealed in argon ambient at 800 °C for 30 min. We have shown in our previous paper that thermal annealing can remove the interstitial zinc out of MgZnO alloys effectively [21]. If the excess zinc really contributes to the conduction of the degenerated $Mg_{0.46}Zn_{0.54}O$ films, the removal of excess zinc will lead to a drastic decrease of the electron concentration in the $Mg_{0.46}Zn_{0.54}O$ films. Experimentally, the electron concentration of the annealed film decreases to 6.5×10^{16} cm^{-3}, which is over two orders of magnitude smaller than that of the as-grown film (1.0×10^{19} cm^{-3}). The above fact confirms that the excess zinc has really contributed to the high electron concentration in the $Mg_{0.46}Zn_{0.54}O$ films, and after the annealing process, the excess zinc comes out from the films. Then one can speculate that the zinc content should be decreased, while the bandgap of the film will change little after the annealing process. In fact, the zinc content in the films decreases from 0.54 to 0.45, while the absorption edge almost remains unchanged after the annealing process, as shown in Fig. 4. Here, inserting the Mg composition of 0.55 Eq. (2), a bandgap of 4.322 eV can be derived, which is in reasonable agreement with the one obtained from the absorption spectrum (4.344 eV). The above phenomenon indicates doubtlessly that the excess zinc is the cause of the high electron concentration in the degenerated MgZnO films.

4. Conclusion

In summary, by introducing excess zinc during the growth process, degenerated $Mg_{0.46}Zn_{0.54}O$ films have been prepared without using any extrinsic dopants. The resistivity of the films can reach 0.053 Ω cm and the electron concentration is as high as 1.0×10^{19} cm^{-3}. The results reported in this paper provides a way to conductive degenerated MgZnO films; thus they may lay a

ground for the fabrication of ZnO-based heterostructured optoelectronic devices or deep ultraviolet devices.

Acknowledgment

This work is supported by National Basic Research Program of China (2011CB302002), the National Natural Science Foundation of China (11134009, 61177040, 11074248, 10974197), and the Science and Technology Developing Project of Jilin Province (20111801).

References

[1] C.W. Lai, J. Zoch, A.C. Gossard, D.S. Chemla, Science 303 (2004) 503.
[2] A. Sandhu, Nature Photonics 1 (2007) 38.
[3] Y. Raniyasu, M. Kasu, T. Makimoto, Nature 441 (2006) 325.
[4] U. Ozgur, Y.I. Alivov, C. Liu, A. Teke, M.A. Reshchikov, S. Dogan, V. Avrutin, S.J. Cho, H. Morkoc, Journal of Applied Physics 98 (2005) 041301.
[5] Y.F. Chen, D.M. Bagnall, Z.Q. Zhu, T. Sekiuchi, K.T. Park, K. Hiraga, T. Yao, S. Koyama, M.Y. Shen, T. Goto, Journal of Crystal Growth 181 (1997) 165.
[6] A. Ohtomo, M. Kawasaki, T. Koida, K. Masubuchi, H. Koinuma, Y. Sakurai, Y. Yoshida, T. Yasuda, Y. Segawa, Applied Physics Letters 72 (1998) 2466.
[7] L.K. Wang, Z.G. Ju, C.X. Shan, J. Zheng, B.H. Li, Z.Z. Zhang, B. Yao, D.X. Zhao, D.Z. Shen, J.Y. Zhang, Journal of Crystal Growth 312 (2010) 875.
[8] H. Zhu, C.X. Shan, B.H. Li, Z.Z. Zhang, B. Yao, D.Z. Shen, Applied Physics Letters 99 (2011) 101110.
[9] Y.N. Hou, Z.X. Mei, Z.L. Liu, T.C. Zhang, X.L. Du, Applied Physics Letters 98 (2011) 103506.
[10] C. Harada, H.J. Ko, H. Makino, T. Yao, Materials Science in Semiconductor Processing 6 (2003) 539.
[11] K.P. Hsueh, Y.C. Cheng, W.Y. Lin, H.C. Chiu, Y.P. Huang, G.C. Chi, W.S. Liu, Proceedings of SPIE 8110 (2011) 81100X.
[12] N.F. Mott, Reviews of Modern Physics 40 (1968) 677.
[13] T. Hirai, Y. Harada, S. Hashimoto, T. Itoh, N. Ohno, Journal of Luminescence 112 (2005) 196.
[14] D.C. Look, R.C. Scott, K.D. Leedy, B. Bayraktaroglu, Proceedings of SPIE 7940 (2011) 794003.
[15] D.K. Ferry, Physical Review B 17 (1978) 912.
[16] E. Ziegler, A. Heinrich, H. Oppermann, G. Stover, Physica Status Solidi A 66 (1981) 635.
[17] K.I. Hagemark, L.C. Chacka, Journal of Solid State Chemistry 15 (1975) 261.
[18] T.A. Krajewski, K. Dybko, G. Luka, L. Wachnicki, B.S. Witkowski, A. Duzynska, K. Kopalko, E. Lusakowska, B.J. Kowalski, M. Godlewski, E. Guziewicz, Physica Status Solidi B 247 (2010) 1653.
[19] C.X. Wu, Y.M. Lu, D.Z. Shen, X.W. Fan, Chinese Science Bulletin 55 (2010) 90.
[20] F. Oba, S.R. Nishitani, S. Isotani, H. Adachi, I. Tanake, Journal of Applied Physics 90 (2001) 824.
[21] Z.G. Ju, C.X. Shan, C.L. Yang, J.Y. Zhang, B. Yao, D.X. Zhao, D.Z. Shen, X.W. Fan, Applied Physics Letters 94 (2009) 101902.